

## Deuteron effects in nucleon-nucleus scattering at intermediate energies

H. F. Arellano

*Department of Physics and Astronomy, University of Georgia, Athens, Georgia 30602  
and Departamento de Física, Facultad de Ciencias Físicas y Matemáticas, Universidad de Chile,  
Casilla 487-3, Santiago, Chile*

F. A. Brieva

*Departamento de Física, Facultad de Ciencias Físicas y Matemáticas Universidad de Chile, Casilla 487-3, Santiago, Chile*

W. G. Love

*Department of Physics and Astronomy, University of Georgia, Athens, Georgia 30602*

(Received 6 April 1994)

We investigate the role of the full dynamical dependence of the free off-shell nucleon-nucleon  $t$  matrix on the optical potential for proton-nucleus elastic scattering in the 100–400 MeV incident energy range within a full-folding model context. Particular emphasis is placed on the effects of deuteron formation by explicitly taking into account pole singularities in the free nucleon-nucleon  $t$  matrix. The full-folding model for the optical potential provides a flexible framework for this purpose as it allows the sampling of the internucleon effective force both off shell and as a function of the energy available in the center of mass for the interacting nucleon pair. A comparison of calculated and measured scattering observables for proton elastic scattering on  $^{40}\text{Ca}$  and  $^{208}\text{Pb}$  leads to the conclusion that the full off-shell free  $t$  matrix is a poor approximation for that part of the nucleon-nucleon effective force required for calculating optical potentials below  $\sim 250$  MeV. Medium effects and higher order corrections to the optical potential are necessary to improve our understanding of nucleon scattering.

PACS number(s): 25.40.Cm, 24.70.+s, 24.10.Ht

### I. INTRODUCTION

A problem systematically eluded in microscopic calculations of nuclear processes is the full account of the bare nucleon-nucleon (NN) force used in deriving the effective NN interaction. Indeed, the presence of a strong resonance in the  $^1S_0$  state and the pole singularity in the  $^3S_1 - ^3D_1$  (deuteron) coupled states in the NN free transition matrix ( $t$  matrix) [1] are not usually considered in the development of widely used effective NN forces [2–6]. Resonances and bound states are treated in detail and, in fact, often play a preeminent role in calculations of few-body problems [7, 8]. One of the main justifications for ignoring these irregular aspects of the NN force is that medium effects are expected [9, 10] to modify the characteristics of the free  $t$  matrix so that its singular properties will not be relevant for nucleons interacting in the nuclear medium. This has been particularly true in the case of local coordinate space models for the NN effective interaction where the localization prescription implies averages of the dynamics over a limited region of phase space [2–4, 6]. Similarly, most theoretical models of the optical potential are normally developed so as to manifestly avoid the singular properties present in the NN effective force, thus providing a plausible though somewhat arbitrary starting point upon which to calculate higher order corrections.

Intermediate energy ( $\sim 200$ –400 MeV) nucleon-nucleus (NA) elastic scattering provides an interesting region

where the importance of the full dynamical complexities of the internucleon effective force may be assessed. At these energies, it has been estimated that medium effects are not too important and therefore the free  $t$  matrix should be a good approximation to the effective force between nucleons [11–14]. At beam energies above 400 MeV the validity of a static nonrelativistic representation for the bare NN force which gives rise to the  $t$  matrix [13, 14] becomes questionable. From a theoretical point of view, the full-folding approach [13] to calculating the NA optical potential provides a framework where we can explore the NN  $t$  matrix both off the energy shell and as a function of the energy available in the center of mass (c.m.) of the interacting nucleon pair [15]. Alternative approaches [11, 12, 14] to calculate NA scattering observables are essentially based on much simpler (factorized)  $t\rho$  approximations to the NA optical potential. In these alternative approaches, the underlying assumption is that the effective force has a smooth energy and off-shell dependence so that the relevant matrix elements needed to determine the optical potential are those corresponding, on average, to the on-shell values of the  $t$  matrix. Clearly in this scheme the presence of bound state(s) and resonances in the NN subsystem are not treated explicitly thereby limiting substantially any assessment of the range of validity of the  $t\rho$  approach. The smooth behavior hypothesis of the  $t$  matrix has been carried forward to estimate higher order terms in a multiple scattering expansion with reasonable success to describe

the experimental data [16, 17]. However, that framework does not identify explicitly the physical mechanisms responsible for smoothing the effective force.

In this paper we investigate implications of a relatively complete treatment of the underlying NN free  $t$  matrix on proton elastic scattering observables in the 100–400 MeV incident energy region. Thus we expect to establish more definitive limits than have been obtained previously for the validity of an effective NN force when neither medium corrections are accounted for nor higher order processes are included. In particular, we shall be able to identify deuteron formation in the target and quantify its effect on the optical potential.

We use the full-folding model approach to calculate the NA optical potential [13]. This model involves basically a convolution of the target ground state mixed density with the off-energy-shell, energy-dependent NN  $t$  matrix. Therefore, the interplay between the incident nucleon energy and the sampling of the effective force by the bound nucleons wave functions will determine how sensitive the scattering process is to the singularities of the  $t$  matrix. A restricted approach was followed in our earlier work [13] where the full energy dependence of the  $t$  matrix was not explicitly accounted for under the assumption that the overlap between the target density and the effective force was negligible in the NN negative energy region. Nevertheless, indirect evidence of the deuteron singularity affecting the NA optical potential was reported in Ref. [15] where a notable sensitivity of the scattering observables to the starting energy was reported.

The outline of this paper is as follows. In Sec. II we briefly present the full-folding model and discuss the role of the deuteron channel in NA scattering calculations. In particular, we show simple estimates of the energy at which the deuteron plays a role under the free  $t$ -matrix assumption for the NN effective force. In Sec. III we compare results from the unrestricted full-folding model with measured observables for proton scattering on  $^{40}\text{Ca}$  and  $^{208}\text{Pb}$  in the 100–400 MeV energy region. Moreover, we show how deuteron formation in the nucleus affects the NA elastic channel and the corresponding absorptive component of the optical potential. Starting energy effects are also discussed within this new framework. Finally in Sec. IV we present a summary of our results and state our conclusions.

## II. THEORETICAL FRAMEWORK AND ESTIMATES

The nonrelativistic description of NA elastic scattering relies on the existence of a bare NN force which provides a reasonably good description of the observables for a two-nucleon system. Based on this bare NN interaction, the idea is to construct an effective force which accounts for the propagation of the nucleon in the nucleus while interacting with the other nucleons in the target and allowing for those nuclear excitations consistent with the elastic process [18–21]. In the intermediate energy region, say nucleon incident energy  $E$  of the order of 200 MeV and above, it is expected that intrinsic medium corrections such as Pauli blocking and the mean nuclear field for the

nucleons are small enough so as to assume that as a reasonable first approximation the effective NN force can be identified with the free  $t$  matrix. As the energy of the incident nucleon decreases, this picture of the scattering process should start slowly deteriorating. However, recent factorized  $t\rho$  calculations suggest that a free NN  $t$  matrix could be reasonably used for nucleon scattering as low as 100 MeV [17]. Within factorized  $t\rho$  approaches binding effects associated with the struck nucleon seem to have little effect on the optical potential.

In principle, a major problem arises in treating the dynamics of NN effective forces. Indeed, the NN free  $t$  matrix shows a resonance near threshold for the  $^1S_0$  state and a pole singularity below threshold due to the existence of the deuteron state in the neutron-proton channel. Therefore, full-folding calculations require an accurate sampling of the  $t$  matrix in order to assess the importance of such effects in the scattering observables. A limited sampling of the  $t$  matrix may miss important contributions of the force, as happens in the factorized  $t\rho$  approximation to the NA optical potential.

In this section we discuss briefly our approach to calculating the NA optical potential. We also make some estimates about the range of energies where the singularities of the  $t$  matrix do not influence this potential significantly.

### A. The full-folding model

The momentum-space representation of the first order optical potential  $U$  for a nucleon of energy  $E$  being scattered by a target can be written as the antisymmetrized matrix elements of a two-nucleon effective force  $T$  [19–21],

$$U(\mathbf{k}', \mathbf{k}; E) = \sum_{\alpha \leq \epsilon_F} \langle \mathbf{k}'; \phi_\alpha | T(E + \epsilon_\alpha) | \mathbf{k}; \phi_\alpha \rangle_A, \quad (1)$$

where  $\{\phi_\alpha\}$  are the single-particle wave functions describing the target nucleus,  $\epsilon_\alpha$  are the corresponding single-particle energies, and  $\epsilon_F$  is the Fermi level for the nucleus. Assuming that medium effects are not important [14], the two-body  $T$  matrix is given by

$$\begin{aligned} & \langle \mathbf{k}', \mathbf{p}' | T(\omega) | \mathbf{k}, \mathbf{p} \rangle \\ &= \delta[(\mathbf{k} + \mathbf{p}) - (\mathbf{k}' + \mathbf{p}')] \\ & \quad \times \langle \frac{1}{2}(\mathbf{k}' - \mathbf{p}') | t_{|\mathbf{k}+\mathbf{p}|}(\omega) | \frac{1}{2}(\mathbf{k} - \mathbf{p}) \rangle, \end{aligned} \quad (2)$$

with the  $\delta$  function making explicit the translational invariance of the two interacting free nucleons and  $t(\omega)$  is the one-body reduced  $t$  matrix defined by [1]

$$\begin{aligned} & \langle \boldsymbol{\kappa}' | t_{\mathbf{Q}}(\omega) | \boldsymbol{\kappa} \rangle \\ &= \langle \boldsymbol{\kappa}' | V | \boldsymbol{\kappa} \rangle + \langle \boldsymbol{\kappa}' | V \frac{1}{\omega - \frac{Q^2}{4m} - K - V + i\eta} V | \boldsymbol{\kappa} \rangle. \end{aligned} \quad (3)$$

Here,  $\boldsymbol{\kappa}$  and  $\mathbf{Q}$  are the relative and c.m. momenta of the nucleon pair,  $V$  is the bare NN force,  $K$  is the relative

kinetic energy operator,  $m$  is the nucleon mass,  $\hbar = 1$  and  $\eta = 0^+$  to have the proper asymptotic conditions for particle propagation. We have chosen to write the explicit solution for the reduced  $t$  matrix rather than its usual Lippmann-Schwinger integral equation [1] to emphasize the presence of the deuteron bound state in our later discussion.

A final expression for the full-folding optical potential can be cast in closed form by inserting Eq. (2) into Eq. (1) and integrating to eliminate the total momentum conserving  $\delta$  function. Replacing the single-particle energies  $\epsilon_\alpha$  by the average binding energy of the nucleons in the target  $\bar{\epsilon}$ , an approximation which does not alter significantly the sampling of the  $t$  matrix [13], we obtain

$$U(\mathbf{k}', \mathbf{k}; E) = \int d\mathbf{P} \rho(\mathbf{q}, \mathbf{P}) \langle \frac{1}{2}(\mathbf{k}' - \mathbf{p}') | t_{|\mathbf{K}+\mathbf{P}|}(E + \bar{\epsilon}) \times | \frac{1}{2}(\mathbf{k} - \mathbf{p}) \rangle_A, \quad (4)$$

with the different momenta defined as

$$\begin{aligned} \mathbf{K} &= \frac{1}{2}(\mathbf{k} + \mathbf{k}'), \\ \mathbf{q} &= \mathbf{k} - \mathbf{k}', \\ \mathbf{p} &= \mathbf{P} - \frac{1}{2}\mathbf{q}, \\ \mathbf{p}' &= \mathbf{P} + \frac{1}{2}\mathbf{q}, \end{aligned} \quad (5)$$

and

$$\rho(\mathbf{q}, \mathbf{P}) = \sum_{\alpha \leq \epsilon_F} \phi_\alpha^\dagger(\mathbf{P} + \frac{1}{2}\mathbf{q}) \phi_\alpha(\mathbf{P} - \frac{1}{2}\mathbf{q}), \quad (6)$$

the target ground state mixed density.

Equation (4) shows the advantage of the full-folding approach. The dynamical characteristics of the NN reduced  $t$  matrix are fully sampled off-shell by the Fermi motion of the nucleons in the target and at the corresponding unrestricted values of the energy available in the c.m. for the NN collision. In actual calculations, the optical potential  $U$  is expressed in terms of its central and spin-orbit components. For proton elastic scattering from closed-shell nuclei, each component of the potential is calculated using the proton-proton and proton-neutron combinations of the  $t$  matrix folded with the correspond-

ing proton and neutron densities. The details can be found in Ref. [13].

One further simplification has been introduced in our present calculations of the optical potential  $U$ . This is related to approximating the mixed density by [22]

$$\begin{aligned} \rho(\mathbf{q}, \mathbf{P}) &\approx \rho(q, P) \\ &\approx \int d\mathbf{R} \rho(\mathbf{R}) e^{i\mathbf{q}\cdot\mathbf{R}} \frac{1}{\hat{\rho}(R)} \Theta[\hat{k}(R) - P], \end{aligned} \quad (7)$$

with  $\rho(R)$  the nucleon density of the target,  $\hat{k}(R)$  determined by either the Slater or Campi-Bouyssy prescriptions [23], and

$$\hat{\rho}(R) = \frac{2}{3\pi^2} \hat{k}^3(R). \quad (8)$$

This has been shown to provide a reasonable representation of the mixed density [22].

## B. Estimates

In order to gain some insight on the role of the  $t$  matrix in the full-folding model, let us make explicit some of the characteristics of the NN free  $t$  matrix. From Eq. (3) it is straightforward to obtain a spectral representation of the  $t$  matrix [1],

$$\begin{aligned} \langle \kappa' | t_{\mathbf{Q}}(\omega) | \kappa \rangle &= \langle \kappa' | V | \kappa \rangle \\ &+ \frac{\langle \kappa' | V | \psi_D \rangle \langle \psi_D | V | \kappa \rangle}{\omega - \frac{Q^2}{4m} - E_D + i\eta} \\ &+ \int_0^\infty dz \frac{\langle \kappa' | V | \psi_z \rangle \langle \psi_z | V | \kappa \rangle}{\omega - \frac{Q^2}{4m} - z + i\eta}, \end{aligned} \quad (9)$$

where  $\psi_D$  is the deuteron wave function,  $-E_D$  is the deuteron binding energy, and  $\psi_z$  is the scattering wave function for the nucleon pair at energy  $z$  in the c.m.

The real part of the  $t$  matrix is given by

$$\text{Re}\{\langle \kappa' | t_{\mathbf{Q}}(\omega) | \kappa \rangle\} = \langle \kappa' | V | \kappa \rangle + \mathcal{P} \frac{\langle \kappa' | V | \psi_D \rangle \langle \psi_D | V | \kappa \rangle}{\omega - \frac{Q^2}{4m} - E_D} + \mathcal{P} \int_0^\infty dz \frac{\langle \kappa' | V | \psi_z \rangle \langle \psi_z | V | \kappa \rangle}{\omega - \frac{Q^2}{4m} - z}, \quad (10)$$

with  $\mathcal{P}$  standing for a principal value prescription to evaluate the force. The imaginary part of the  $t$  matrix is given by

$$\text{Im}\{\langle \kappa' | t_{\mathbf{Q}}(\omega) | \kappa \rangle\} = -i\pi\delta\left(\omega - \frac{Q^2}{4m} - E_D\right) \langle \kappa' | V | \psi_D \rangle \langle \psi_D | V | \kappa \rangle - i\pi\Theta\left(\omega - \frac{Q^2}{4m}\right) \langle \kappa' | V | \psi_{z_0} \rangle \langle \psi_{z_0} | V | \kappa \rangle, \quad (11)$$

where  $z_0 = \omega - \frac{Q^2}{4m}$ . The above spectral decomposition prescribes explicitly how the full-folding model should take into account the presence of the deuteron pole when the  $t$  matrix is folded with the target density. In particular, an extra contribution to the absorption comes from the residue at the deuteron pole. This fact is physically

significant since it corresponds to loss of flux from the elastic channel due to deuteron formation in the nuclear medium. Whether this process contributes significantly to elastic scattering remains to be tested. We shall address this issue in the next section where we compare the results of our calculations to actual experimental data.

Two comments seem appropriate here. One is related to the ability of the full-folding model to genuinely explore the complexities involved in the NN  $t$  matrix and thus incorporate explicitly new physics in the calculation of the optical potential. The other refers to the questionable validity of the assumptions behind approximate first-order models such as the on-shell and off-shell  $t\rho$  models [11, 12, 14] which ignore the importance of the energy dependence of the force.

To remark on the energy dependence of the  $t$  matrix around the threshold region [ $\omega \approx \frac{Q^2}{4m}$  in Eq. (11)], we have considered a particular matrix element corresponding to forward scattering  $\kappa' = \kappa$  and  $\kappa = \frac{1}{2}\sqrt{2m\omega}$ . In Fig. 1 we have plotted the real and imaginary parts of  $t_{pp}$  (proton-proton) and  $t_{pn}$  (proton-neutron) components of the central effective force as a function of the c.m. energy ( $\omega - \frac{Q^2}{4m}$ ) for a starting energy of  $\omega = 160$  MeV. Thus we display the NN interaction over an important region where matrix elements of the force are required by the full-folding model. In the  $pp$  channel we clearly observe a strong though localized energy dependence near threshold which is due to the  $^1S_0$  state. In the  $pn$  channel, the real part of the force is dominated by the presence of the deuteron singularity, generating a region of strong cancellations when the interaction is folded with the density.

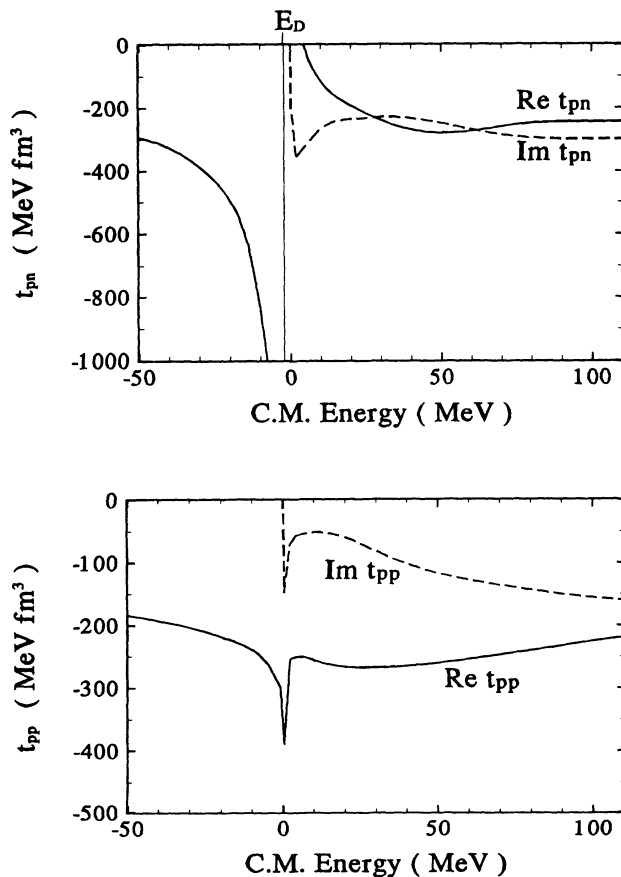


FIG. 1. Behavior of the central component of the free  $t$  matrix as a function of the NN c.m. energy. The upper and lower frames correspond to the  $pn$  and  $pp$  channels, respectively.  $-E_D$  corresponds to the deuteron binding energy.

Overall the  $t$  matrix is smoothly energy dependent except in the threshold and deuteron bound state region. The extent to which this region is important in determining the optical potential will depend on the energy of the incident nucleon and the range of the mixed density [Eq. (4)] in momentum space.

A simple overall picture of the importance of the deuteron channel within a free  $t$ -matrix approximation for the effective NN interaction can be illustrated by considering the forward on-shell matrix element of the optical potential. From Eqs. (4) and (5) we have

$$U(\mathbf{k}_0, \mathbf{k}_0; E) = \int d\mathbf{P} \rho(0, \mathbf{P}) \langle \frac{1}{2}(\mathbf{k}_0 - \mathbf{P}) | t_{|\mathbf{k}_0 + \mathbf{P}|}(E + \bar{\epsilon}) \times | \frac{1}{2}(\mathbf{k}_0 - \mathbf{P}) \rangle_A, \quad (12)$$

where  $|\mathbf{k}_0| = k_0 = \sqrt{2mE}$ . Realizing that the momentum distribution of the mixed density varies essentially between  $0 \leq P \leq P_{\max}$ , with  $P_{\max} \approx 1.4 \text{ fm}^{-1}$ , then the c.m. momentum will vary between  $\max\{0, k_0 - P_{\max}\}$  and  $(k_0 + P_{\max})$ . On the other hand, the values of the c.m. momentum  $Q_D$  at which the  $t$  matrix becomes singular are given by

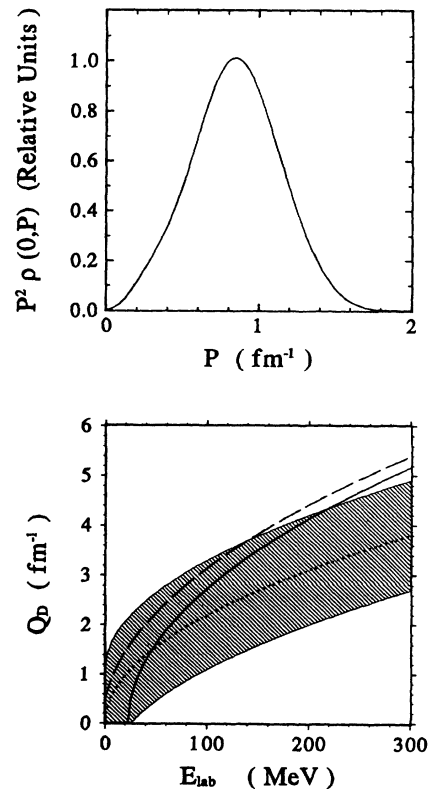


FIG. 2. Upper frame: momentum profile of the ground state mixed density for nucleons in  $^{40}\text{Ca}$  at  $q = 0$ . Lower frame: NN c.m. momentum for the deuteron bound state as a function of the energy of the projectile. The solid and dashed curves correspond to situations where  $\bar{\epsilon} = -25$  MeV and  $\bar{\epsilon} = 0$ , respectively. The dotted curve represents the on-shell momentum of the projectile. The shaded area shows the range in  $P$  relevant to the forward on-shell matrix element of the optical potential [see Eq. (12)].

$$E + \bar{\epsilon} - \frac{1}{4\pi} Q_D^2 - E_D = 0. \quad (13)$$

In the upper frame of Fig. 2 we show, as a function of the average struck nucleon momentum  $P$ , the momentum profile of the mixed density at  $q = 0$  given by  $P^2 \rho(0, P)$ . We observe that the momentum distribution extends up to around  $\sim 1.5 \text{ fm}^{-1}$ , therefore setting the boundaries for off-shell and energy sampling of the effective force. In the lower frame we present the range of variation of the c.m. momentum for a typical value of  $P_{\text{max}} = 1.1 \text{ fm}^{-1}$  which corresponds to roughly half density in the nucleus. This range is represented by the shaded region around  $Q = k_0(E)$  (dotted curve). Also in Fig. 2 we plot  $Q_D(E)$  for an average nucleon binding of  $\bar{\epsilon} = 0$  (dashed curve) and  $\bar{\epsilon} = -25 \text{ MeV}$  (full curve). A clear and simple picture emerges. Where the solid or dashed curve intersects the shaded region, the full-folding model requires matrix elements of the force throughout the energy region where deuteron formation exists. Conservatively we observe that only above 200 MeV the singular features of the  $t$  matrix will not be strongly sampled. As the incident energy decreases below 200 MeV the situation

changes considerably and a more careful treatment of the deuteron becomes essential. A precise estimate of the critical energy depends on the choice of the average energy  $\epsilon$  as observed by Crespo and collaborators [24].

A final comment is necessary concerning some full-folding calculations we have reported previously [13, 15]. There the  $t$  matrix used for negative NN c.m. energies was obtained by extrapolating those calculated in the positive energy region thus effectively underplaying the role of the deuteron. However, since most of the results were for proton energies of 200 MeV and above, the density did not essentially sample the singular region and therefore our findings are practically correct. Under the same considerations our results of Ref. [13] for 135 MeV protons on  $^{16}\text{O}$  do not adequately represent all of the physics contained in the full-folding model.

### III. ELASTIC SCATTERING OBSERVABLES

The full-folding optical potential [Eqs. (4) and (7)] was calculated following the general procedure outlined in Ref. [13]. To account properly for the presence of

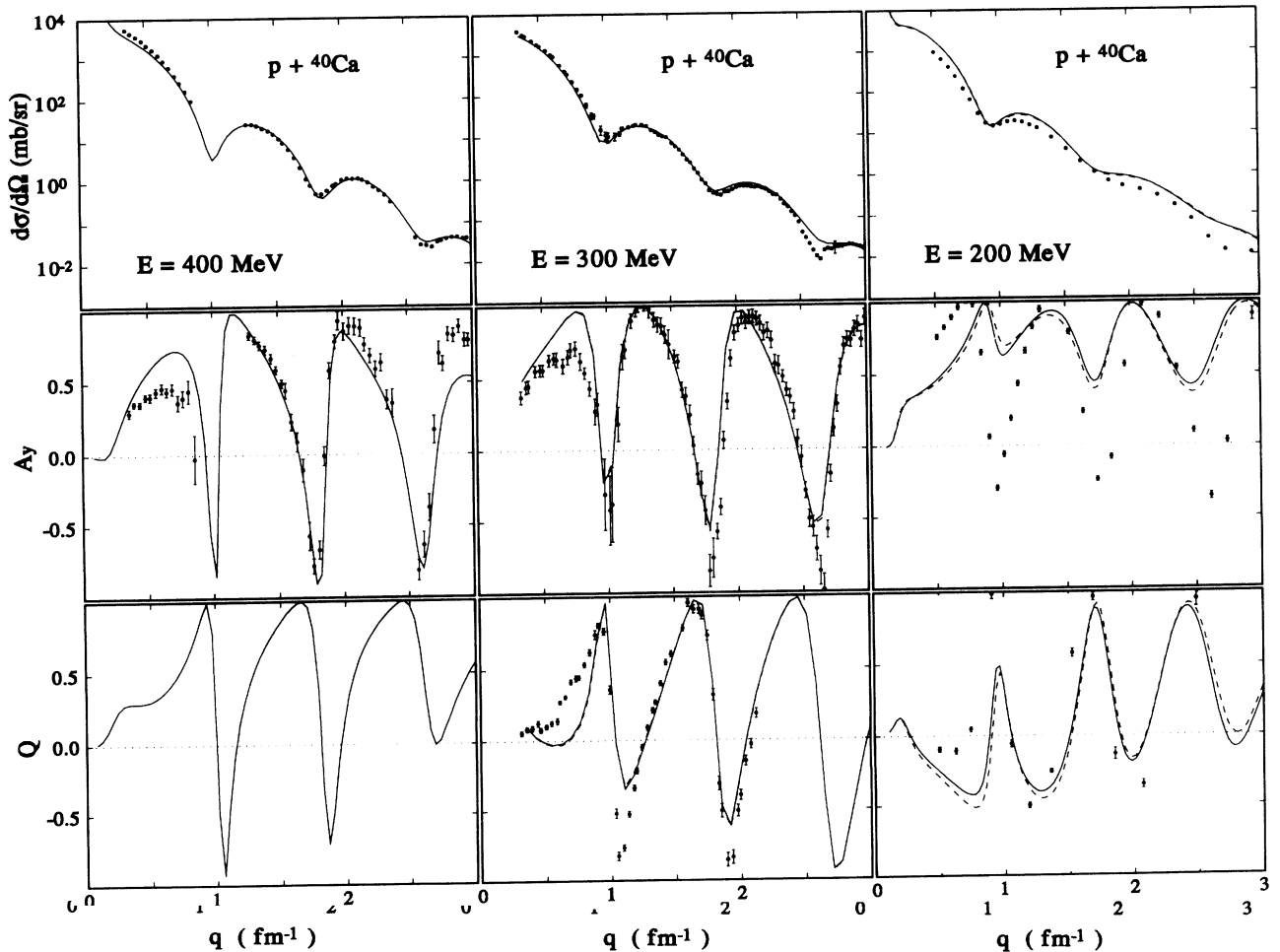


FIG. 3. Calculated and measured elastic scattering observables for  $p+^{40}\text{Ca}$  at 400, 300, and 200 MeV. The solid curves represent full-folding results. The dashed curves correspond to full-folding results neglecting the deuteron absorptive contribution. See text for references to the data.

the deuteron bound state in the  $t$  matrix we have extended our computing codes in order to evaluate the corresponding principal value integral and the pole residue contribution to the absorption [Eqs. (12) and (13)].

The NN  $t$  matrix was calculated from the Paris potential [25] using standard matrix inversion methods. The residue at the deuteron pole was calculated using a finite albeit very small  $\eta$  in the two-nucleon propagator of Eq. (3). The procedure has proven to be very stable and accurate.

Calculations of differential cross sections ( $d\sigma/d\Omega$ ), analyzing powers ( $A_y$ ) and spin rotation functions ( $Q$ ) were made for proton elastic scattering on  $^{40}\text{Ca}$  and  $^{208}\text{Pb}$  at energies between 100 and 400 MeV. Coulomb scattering was treated as described in Ref. [13]. By exploring this range of energies, where we compare theoretical results with data, we can set practical bounds for the validity of the free NN  $t$  matrix in the context of the full-folding model.

The target density for  $^{40}\text{Ca}$  was determined from a single-particle model using a Wood-Saxon parametrization for the mean field designed to fit the rms radius of the point-proton density determined from electron scattering and to fit experimental single-particle energies [13]. The average binding energies were  $-24.0$  and  $-31.4$  MeV for

protons and neutrons, respectively. In practice we have used the same average binding for both protons and neutrons,  $\bar{\epsilon} = \frac{1}{A}(Z\bar{\epsilon}_p + N\bar{\epsilon}_n) = -27.7$  MeV, with  $Z$  the proton number and  $N$  the neutron number and  $A = Z + N$ . In the case of  $^{208}\text{Pb}$  the target density was determined from Ref. [26], giving an overall average binding energy  $\bar{\epsilon} = -24.0$  MeV.

In Figs. 3 and 4 we present measured and calculated observables for  $p+^{40}\text{Ca}$  elastic scattering at 400, 300, 200, 181, and 160 MeV as a function of the momentum transfer. Measurements of  $d\sigma/d\Omega$  and  $A_y$  at 400 and 300 MeV have been reported in Ref. [27]. Spin rotation measurements shown at 300 MeV correspond to an actual beam energy of 320 MeV and were taken from Ref. [28]. The data at 200 MeV are from Ref. [29]. The cross-section data at 181 and 160 MeV were taken from Refs. [30] and [31], respectively, whereas the corresponding  $A_y$  data are from Refs. [31] and [32], respectively. The full curves represent the complete full-folding calculations while the dashed curves show the case when the absorption generated by deuteron formation [first term in Eq. (11)] is omitted. At 300 and 400 MeV the agreement between theory and experiment is very good and of quality similar to results reported earlier [13]. At these energies the sampling of the singular part of the  $t$  matrix is very weak and

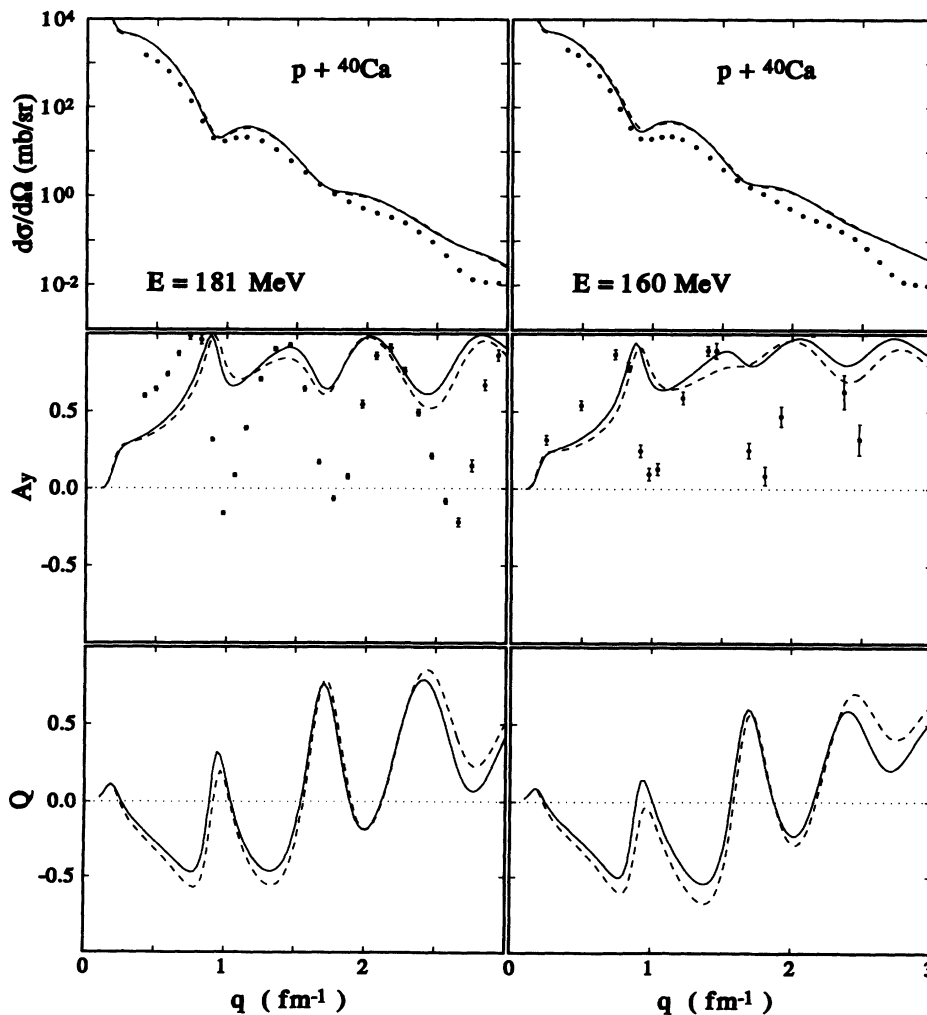


FIG. 4. Same as Fig. 3 but for  $p+^{40}\text{Ca}$  at 181 and 160 MeV. See text for references to the data.

therefore differences between the full and dashed curves are not noticeable. At these higher energies our conclusions regarding differences between full-folding and  $t\rho$  calculations are unaltered from those reached in Ref. [13].

At 200 MeV the agreement between the calculated observables and the data begins to deteriorate especially for the spin observables. Indeed, as estimated in Sec. II B, this energy sets roughly the boundary where the  $^1S_0$  resonance and the deuteron bound state in the force start modifying the optical potential. At this energy we also see differences depending on whether the absorption due to the deuterons is included or not. As the proton incident energy decreases the disagreement between theory and experiment increases notably for both the cross-sections and spin observables.

In Figs. 5 and 6 we present the results of our calculations for  $p+^{208}\text{Pb}$  elastic scattering at 400, 300, 200, 160, 121, and 98 MeV as a function of the momentum transfer. Full-folding model results for this target have not been reported. The data for the scattering observables at beam energies of 400, 300, and 200 MeV are from Ref. (27). The corresponding measurements at 160 and 121 MeV are reported in Ref. [32], whereas the 98-MeV data

are reported in Ref. [31]. The meaning of the full and dashed curves follows the discussion of Figs. 3 and 4. We observe the same trend as in the  $p+^{40}\text{Ca}$  case. The free  $t$  matrix gives a notably good description of the data at the higher energies. However, when the deuteron singularity becomes significantly sampled around 200 MeV the description of the data quickly worsens both for the cross sections and spin observables.

The question arises as to whether different bare NN forces will alter our findings significantly regarding the role of the deuteron in low energy elastic scattering. We expect that the answer is no since the main differences among reasonable internucleon potentials is in their off-shell behavior but unlikely in their energy dependence near threshold nor at the deuteron binding energy.

We have also investigated the sensitivity of our calculations to the choice of the starting energy. This is important since the starting energy largely determines the extent to which the deuteron region is sampled in the  $t$  matrix. Consequently we have done calculations for  $p+^{208}\text{Pb}$  optical potentials with average nucleon binding energies of  $\bar{\epsilon} = -24.0$  and 0 MeV. Our findings are similar for the  $p+^{40}\text{Ca}$  case. In Fig. 7 we have plotted our results

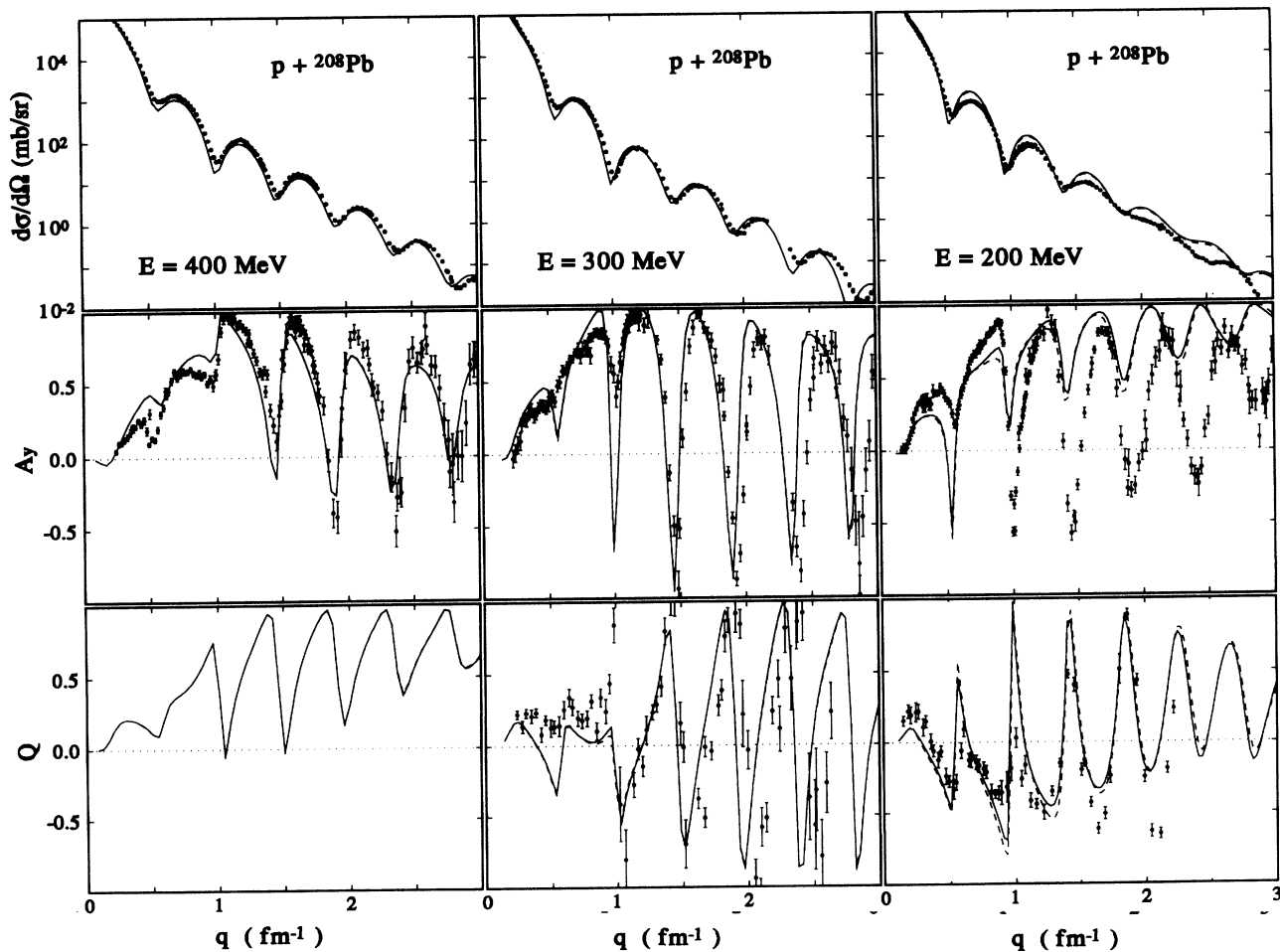


FIG. 5. Calculated and measured elastic scattering observables for  $p+^{208}\text{Pb}$  at 400, 300, and 200 MeV (see text for references to the data). The solid curves represent full-folding results. The dashed curves correspond to full-folding results neglecting the deuteron absorptive contribution.

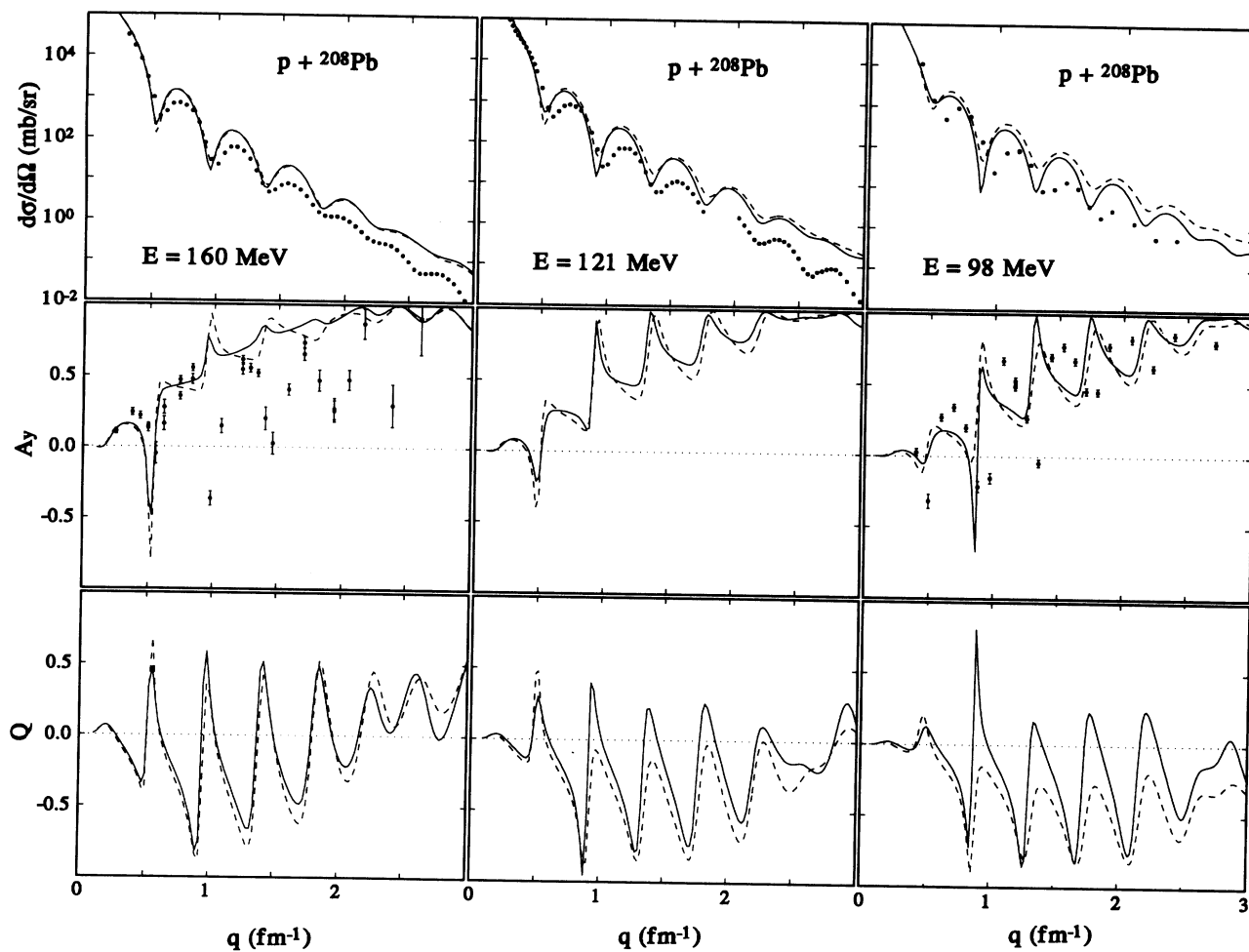


FIG. 6. Same as Fig. 5 but for  $p+^{208}\text{Pb}$  at 160, 121, and 98 MeV. See text for references to the data.

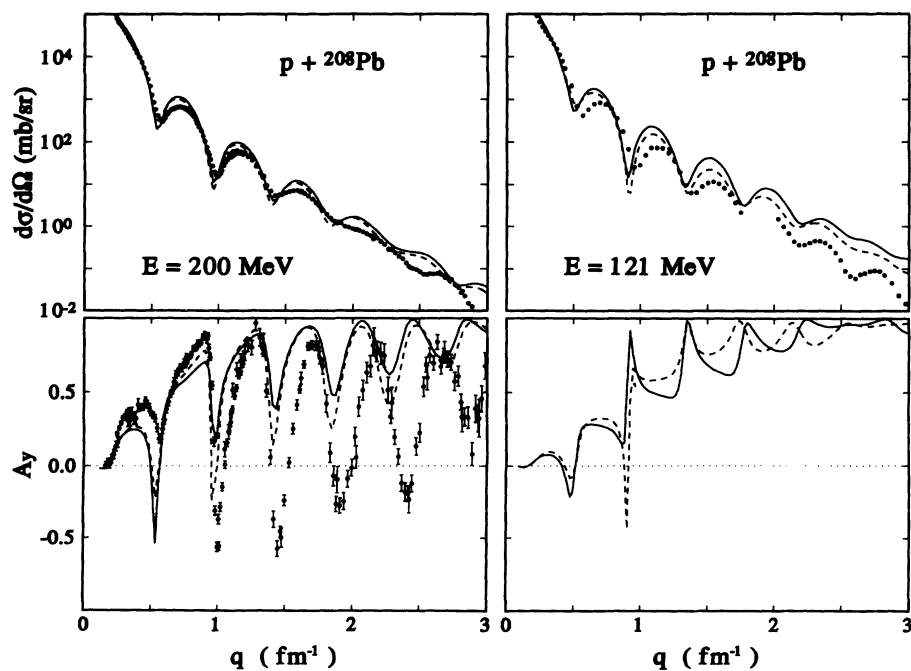


FIG. 7. Starting energy effects in the calculated observables for  $p+^{208}\text{Pb}$  elastic scattering at 200 and 121 MeV. The calculated observables correspond to full-folding calculations using  $\bar{\epsilon} = -24$  MeV (solid curves) and  $\bar{\epsilon} = 0$  (dashed curves) for the starting energy. Both calculations include the deuteron absorptive contribution.

and the data as a reference point for  $E=121.0$  and 200 MeV. The full curves correspond to  $\bar{\epsilon}=-24.0$  MeV and the dashed ones to  $\bar{\epsilon} = 0$ . We observe that there is a strong dependence on the choice of the starting energy with the calculations getting somewhat closer to the data when  $\bar{\epsilon} = 0$ . Our interpretation is that for  $\bar{\epsilon} = 0$  the deuteron contributes less to the matrix elements (roughly the on-shell values) of the optical potential relevant to the scattering observables, signaling that deuteronlike singularities are far less important in determining the scattering process than calculations with a more realistic  $\bar{\epsilon}$  suggest. Rather than changing arbitrarily the starting energy to improve the description of the data, we conclude that medium and/or higher order contributions to the optical potential are quite important even at or above 200 MeV. Indeed, the inclusion of propagation in the presence of a nuclear mean field will tend to push the deuteron singularity away from the overlapping region between the effective force and the density. The recent work of Crespo and collaborators [24], which treats the momentum dependence of the interaction less completely than is done here, indicates that the inclusion of the binding potential for the struck nucleon in the intermediate states shifts the effective  $\bar{\epsilon}$  to positive values. The medium effects included in Ref. [17] lead to an overall reduction in the propagating energy and to small corrections to observables above 100 MeV incident energy. The inclusion of medium-dependent double-scattering terms within an optimal factorization approximation has been shown [16] to have small effects on proton scattering observables above 100 MeV, while generating substantial modifications to proton-nucleus wave functions for small partial waves. Calculations which incorporate medium effects within the full-folding framework are underway [33].

#### IV. CONCLUSIONS

In this paper we have extended earlier full-folding model calculations of the optical potential for NA elastic scattering to include the full range of NN dynamics in order to assess in some detail the role of the free NN  $t$  matrix as the effective internucleon force. In particular, we are now able to incorporate in the full-folding calculations the pole singularity due to the deuteron state present (and the  $^1S_0$  resonance) in the  $t$  matrix.

Within this framework we have estimated that for nucleon energies below  $\sim 250$  MeV, the optical potential requires matrix elements which are strongly influenced by the deuteron bound state in the NN free  $t$  matrix. This result means that the optical potential is very sensitive to the energy available in the c.m. of the interacting nucleon pair, since the target density requires a sampling of the energy region where the  $t$  matrix becomes singular.

The full-folding model provides a flexible framework for exploring these effects. Alternative, more approximate approaches for calculating the optical potential which use the free  $t$  matrix for the effective internucleon force in the energy range we have explored do not treat the strong energy dependence of the NN  $t$  matrix at low energies explicitly. The conclusions obtained using these more approximate approaches are much more restricted and should be interpreted accordingly.

At 300 MeV and above, the full-folding model gives very good results for protons on  $^{40}\text{Ca}$  and  $^{208}\text{Pb}$ . These results are of similar quality to those reported in Ref. [13] and are closer to the data than the results obtained using factorized  $t\rho$  models. Therefore we can conclude that the difference between the full-folding and the  $t\rho$  models directly reflects a more complete sampling of the off-shell properties of the  $t$  matrix in the full-folding model.

At 200 MeV and below we observe a rapid deterioration of the full-folding model when compared to the data. Although the theory yields a strong influence of the singular region in the  $t$  matrix, our results including this region differ considerably from the measured observables. We conclude that the free  $t$  matrix is a poor approximation to the effective NN interaction in nuclei for describing nuclear elastic scattering below  $\sim 200$  MeV.

Our study of the role of the starting energy also shows that the agreement between theory and experiment improves when the starting energy is increased, thus weakening the explicit influence of the deuteron bound state. This suggests that other effects which, among other things effectively dampen the role of the deuteron bound state, must be incorporated into the calculation of the effective NN force to account for the differences between measured and calculated observables shown in Figs. 3–6.

Overall, the present study shows how far we can go with the free  $t$  matrix to understand nucleon-nucleus scattering in a first-order approximation to calculate the corresponding optical potential. Unfortunately the range of energies is not too encouraging: below  $\sim 250$  MeV the theoretical results start failing to account reasonably well for the experimental data and above 400 MeV the bare NN force is not designed to reproduce well the NN physics. Medium effects offer a promising direction for overcoming some of these difficulties.

#### ACKNOWLEDGMENTS

This work was supported in part by NSF Grants Nos. PHY-8903856 and PHY-9143465 and FONDECYT Grants Nos. 1931115 and 3940008. F.A.B. thanks the Department of Physics and Astronomy of the University of Georgia for its hospitality during his visit.

- [1] S. K. Adhikari and K. L. Kowalski, in *Dynamical Collision Theory and Its Applications* (Academic, New York, 1991).
- [2] P. J. Siemens, Nucl. Phys. **A141**, 225 (1970).
- [3] F. A. Brieve and J. R. Rook, Nucl. Phys. **A291**, 317 (1977); **A307**, 493 (1978).

- [4] H. V. von Geramb, in *The Interaction Between Medium Energy Nucleons in Nuclei*, edited by H. O. Meyer (AIP, New York, 1983); L. Rikus and H. V. von Geramb, Nucl. Phys. **A426**, 496 (1984).
- [5] W. G. Love and M. A. Franey, Phys. Rev. C **24**, 1073 (1981).

- [6] K. Nakayama and W. G. Love, *Phys. Rev. C* **38**, 51 (1988).
- [7] C. Lovelace, *Phys. Rev.* **135**, B1225 (1964), and references cited therein.
- [8] A. G. Sitenko, in *Scattering Theory* (Springer-Verlag, New York, 1991), and references cited therein.
- [9] A. A. Ioannides and R. C. Johnson, *Phys. Rev. C* **17**, 1331 (1978).
- [10] B. L. Gambhir and J. J. Griffin, *Phys. Rev. C* **7**, 590 (1973).
- [11] R. Crespo, R. C. Johnson, and J. A. Tostevin, *Phys. Rev. C* **41**, 2257 (1990).
- [12] Ch. Elster, T. Cheon, E. F. Redish, and P. C. Tandy, *Phys. Rev. C* **41**, 814 (1990).
- [13] H. F. Arellano, F. A. Brieva, and W. G. Love, *Phys. Rev. Lett.* **63**, 605 (1989); *Phys. Rev. C* **41**, 2188 (1990).
- [14] L. Ray, G. W. Hoffmann, and W. R. Coker, *Phys. Rep.* **212**, 223 (1992).
- [15] H. F. Arellano, W. G. Love, and F. A. Brieva, *Phys. Rev. C* **43**, 2734 (1991).
- [16] R. Crespo, R. C. Johnson, and J. A. Tostevin, *Phys. Rev. C* **46**, 279 (1992).
- [17] C. R. Chinn, Ch. Elster, and R. M. Thaler, *Phys. Rev. C* **48**, 2956 (1993).
- [18] H. Feshbach, *Ann. Phys. (N.Y.)* **5**, 357 (1958); **19**, 287 (1962).
- [19] A. K. Kerman, H. McManus, and R. M. Thaler, *Ann. Phys. (N.Y.)* **8**, 551 (1959).
- [20] A. L. Fetter and K. M. Watson, in *Advances in Theoretical Physics*, edited by K.A. Brueckner (Academic, New York, 1965), Vol. 1; G. Takeda and K. M. Watson, *Phys. Rev.* **97**, 1336 (1955).
- [21] J. P. Jeukenne, A. Lejune, and C. Mahaux, *Phys. Rep.* **25C**, 83 (1976).
- [22] H. F. Arellano, F. A. Brieva, and W. G. Love, *Phys. Rev. C* **42**, 652 (1990).
- [23] X. Campi and A. Bouyssy, *Phys. Lett.* **73B**, 263 (1978).
- [24] R. Crespo, R. C. Johnson, and J. A. Tostevin, *Phys. Rev. C* **48**, 351 (1993).
- [25] M. Lacombe, B. Loiseau, J. M. Richard, R. Vinh Mau, J. Côté, P. Pirés, and R. de Tourreil, *Phys. Rev. C* **21**, 861 (1980).
- [26] J. W. Negele, *Phys. Rev. C* **1**, 1260 (1970).
- [27] D. A. Hutcheon *et al.*, *Nucl. Phys.* **A483**, 429 (1988).
- [28] E. Bleszynski *et al.*, *Phys. Rev. C* **37**, 1527 (1988).
- [29] E. J. Stephenson, *J. Phys. Soc. Jpn. (Suppl.)* **55**, 316 (1985).
- [30] A. Ingemarsson and G. Tibell, *Phys. Scr.* **4**, 235 (1971).
- [31] P. Schwandt, H. O. Meyer, W. W. Jacobs, A. D. Bacher, S. E. Vidgor, M. D. Kaitchuck, and T. R. Donoghue, *Phys. Rev. C* **26**, 55 (1982).
- [32] A. Nadasen, P. Schwandt, P. P. Singh, W. W. Jacobs, A. D. Bacher, P. T. Debevec, M. D. Kaitchuck, and J. T. Meek, *Phys. Rev. C* **23**, 1023 (1981).
- [33] H. F. Arellano, F. A. Brieva, and W. G. Love (unpublished).